Synergy in Small-World Networks

Candidate Number: 8317R. Supervisor: Dr. S.N. Taraskin

May 12, 2014

Abstract

The spreading processes of diseases, rumours and opinions are often well-approximated by mathematical transmission models. This paper presents a numerical C++ implementation of the Susceptible-Infectious-Removed (SIR) transmission model, often used for modelling the spread of Measles, Mumps and Rubella infections. The implementation accounts for synergistic effects, which cause non-linear correlations between the transmission rates of nearby infected hosts. It also allows for network rewiring, whereby non-adjacent members of the population can share the infection via shortcuts. These shortcuts can be either radius-constrained (finite rewiring) or unconstrained (infinite rewiring). In this paper, we will first discuss the improvements that have been developed since the previous FORTRAN implementation, before presenting the results of our new code. In our results, we discriminate between invasive infections which extend throughout the population, and non-invasive (or localised) infections which affect only small regions of the population. The transition from non-invasive to invasive infections occurs at a critical transmission rate, α_c, such that invasive infections are those with transmission rate $\alpha > \alpha_c$. Our results are in two parts. First, we observed the known effect of infinite network rewiring on the critical transmission rate. Namely, that for infinite network rewiring there is a critical value of the synergy, $\beta_c = (3.0 \pm 0.1)\ s^{-1}$, above which the critical transmission rate counter-intuitively increases with rewiring. An interpretation of this effect is given. Secondly, we observed that a very similar effect occurs for finite rewiring, differing only in the critical synergy values β_c. To our knowledge, these results represent the first time that this effect has been observed for finite rewiring. The critical synergy value, β_c, was found to depend on the range of permitted rewiring radii. For rewiring within 5 to 10 lattice spacings, we observed $\beta_c = (2.0 \pm 0.1)\ s^{-1}$. For rewiring within 10 to 15 lattice spacings, we observed $\beta_c = (2.5 \pm 0.1)\ s^{-1}$. We offer an explanation as to why β_c changes with these different constraints.

1 Introduction

Abstract numerical models are frequently used to model the spread of infections. For instance, the SIR model in this paper has been successfully compared to real disease data for Measles [1], Mumps [2], and Rubella [3], and a closely related model has shown results for rumours spreading in social networks [4].

This distinction between invasive and non-invasive infections is of vital importance when considering what effect a new disease might have on a population. An invasive infection is one that pervades all parts of the population, whereas a non-invasive (or localised) infection is one that affects a small number of smaller regions. Invasive infections have a much more devastating effect, and can determine whether or not the disease will be containable [5].

Also of importance is the effect of network rewiring on invasive behaviour. Network rewiring is the process of creating shortcuts between members of the population (or "nodes") that would otherwise be too distant to share the infection. An examples might be an insect carrying an infection between far-off flowers in a field, or a human transmitting a disease during international travel.

The simple SIR model assumes that each infected host transmits the infection independently of all others: there are no correlations between infected hosts. Advances have been made in such correlations, in particular between the infection rates of nearby hosts. These correlations are known as Synergy and can cause either cooperation (positive synergy) or competition (negative synergy) between nearby infected hosts in their attempt to transmit the infection to other nodes. Synergy is easily understood for the spreading process of a rumour in a social network [6]. Members of the group may wish either to help—or to hinder—the continued transmission of the rumour, depending on their own personal stake in the rumour. Such members will actively interfere with others' attempts to transmit the disease, thereby causing correlations between the transmission rates of nearby hosts. We consider cases where all members of the population have the same synergy.

We will show in this paper that, for a disease or infection where there is strong cooperation between the infected hosts, it is possible to decrease the spread of the disease by increasing the extent of network rewiring.

1.1 Previous work

A previous toy model [7] of SIR transmission with synergy was used as a starting point for our new implementation. Other models had been used to investigate the invasive behaviour of an infection under infinite network rewiring [8], where shortcuts can be created between any two nodes in the network no matter how distant. It was found that an infection can spread much more easily in a rewired network, since the shortcuts provide a fast way of spreading into distant regions of the network. Results generated by the previous toy model have shown that the opposite effect is observed for infections exhibiting strong cooperation (positive synergy) between infected hosts: rewiring was found actually to disrupt the spread of an infection.

These somewhat counter-intuitive results are investigated further in this paper. Additionally, we investigate a more realistic model of finite network rewiring, where shortcut lengths can only lie within some fixed range of radii. These lower- and upper-bounds on the rewiring radii might represent, for instance, the range over which an insect will travel between flowers, or the distance over which an infectious spore will be carried by the wind. Some interest has been shown in the connection between radius of transmission and invasive behaviour, both for plant diseases [9] and for HIV in humans [10].

1.2 Structure

The rest of this paper is split into the following sections. In Section 2, we present the SIR model theory using available literature. Section 3 contains a brief description of our C++ implementation, along with several improvements that have been made over the previous FORTRAN code. Section 4 contains our methodology, and the ways in which we attempted to reduce any potential errors. In Section 5 we present our results of how the invasive behaviour of synergistic infections changes under network rewiring. These data are presented graphically, the main features of which are explained and later discussed in more detail in Section 6. Section 7 contains some overall conclusions, as well as some aspects of our results that would be interesting to investigate further.

2 Theory

2.1 SIR Model

In the SIR Model, each node is in one of three states: Susceptible, Infectious, or Removed. A Susceptible node remains in that state unless it receives the infection from an Infectious neighbour. It then becomes Infectious, and remains in that state for a fixed time (τ) during which it is able to transmit the infection to its Susceptible neighbours. After a node's infectious period is over, it is Removed from the network. The infection is described as extinct when there are no longer any infectious nodes in the network.

2.1.1 Infection Rate and Synergy

The infection spreads from node-to-node according to a Poisson distribution for uncorrelated random events. If Node S has n_s infected neighbours, then the total reaction rate of Node S being infected is given [6] by

$$\lambda = n_s(\alpha + \beta(n_s - 1)) \quad (1)$$

where α is the synergy-free rate of infection, and β is the synergy contribution. In the absence of any other correlations or changes to n_s, the probability that Node S becomes infected after a time t is then $P(t) = 1 - \exp(-\lambda t)$. Hereafter, we will write often α and β without their units (s^{-1}, or Hz).

2.1.2 Network Rewiring

Network rewiring involves the breaking and remaking of bonds in the network. Before rewiring, each node is bonded only to its adjacent nodes so that, on our square lattices, there are four bonds per node. The extent of rewiring in a network is quantified [11] by a rewiring probability, ϕ. Each bond in a network will be rewired with probability ϕ, so that the number of rewired bonds obeys a simple Binomial distribution. A single rewiring event has two steps. First, an existing bond between two nodes is destroyed, such that those two nodes have one fewer neighbour than before. Secondly, a new bond is created from one of those two deficient nodes to a completely different node, possibly faraway. The distant node is selected uniformly from all possible nodes within the constrained radii. The result of one rewiring event is shown schematically in Figure 1. Note the change in coordination numbers (number of neighbours) for each node, as this is key to the interpretation of our results (see Section 6.1).

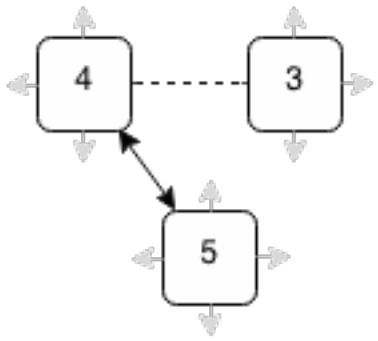

FIGURE 1: Network Rewiring, showing bond destruction (dotted line), bond creation (bold arrow), and the new number of neighbours for each Node (3,4,5)

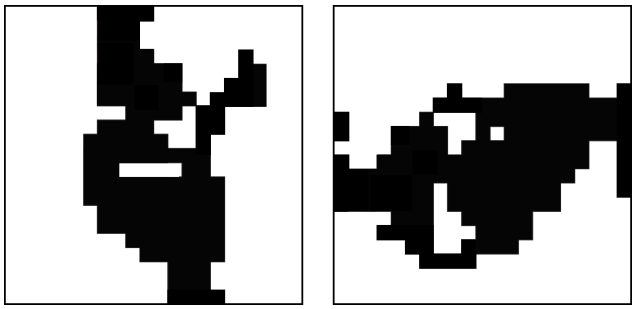

FIGURE 2: Example 1-Dimensional Epidemics: Vertical and Horizontal

2.1.3 Epidemics and Effective Mass

We can classify the final extinction state of an infection as either Epidemic or non-Epidemic. An Epidemic occurs if the infection spans the entire network, from one edge to the other. We concern ourselves only with 1-dimensional epidemics, where the infection spans the network either vertically or horizontally, but not both. Two example cases of 1d epidemics are shown in Figure 2. Unfortunately, our theoretical expectations [6] for how 1d epidemics depend on α is only valid for small-world networks. This forces restrictions on the maximum bond length and bond density of rewiring, and is certainly not valid for the infinite rewiring regime. Instead, we can measure the "Effective Mass" of an extinct infection: the total number of nodes that have been infected as a fraction of the total number of nodes in the network. The effective mass is expected [12] to follow a closely-linear fit near the critical transmission rate, intercepting the Mass = 0 axis at $\alpha = \alpha_c$.

2.2 Errors

The counting of 1d epidemics and the measuring of Effective Mass follow standard error processes [13]. For N realisations of a single network size L, the error in counting epidemics is expected to go as $^1/_{\sqrt{N}}$. We also use a very pessimistic error of $^1/_{\sqrt{N}}$ for measuring the Effective Mass after N realisations. Our lack of confidence in measuring the Effective Mass is due to the strong correlations between the probabilities of two different nodes becoming infected – for singe realisations, the Effective Mass is more often closer to zero or one, than to the intermediate range. The errors associated with measuring effective-gradients (see Section 5) are found by determining the maximum and minimum possible lines of best fit, rather than using the results of linear regression, since the lines in question are not fully linear and the effective-gradients are merely a measure of changes in behaviour.

3 Implementation

In this section, we explain the way in which our implementation causes the infection to progress through time, by using the kinetic Monte Carlo method. The new implementation has significant speed and performance improvements over the previous FORTRAN code [6]. The rationale behind these improvements will also be explained in this section.

3.1 Kinetic Monte Carlo

The Kinetic Monte Carlo (KMC) method is used to model the time progression of randomly occurring processes, where each random event has a well-defined rate of reaction. We recognise a finite number of events e, each of which can occur with some reaction rate λ_e. The KMC method progresses through time in a two step process:

1. Randomly choose the time at which the next event will occur, based on the sum of all reaction rates λ_e
2. Randomly choose one of the events to occur at that time, weighted according to their individual reaction rates

This differs strongly from discrete-time methods where time progresses in fixed time steps and, in each time step, the reaction rate of each event determines whether that event occurred. Such discrete methods neglect correlations between events, where the occurrence of one event during a time step might affect the reaction rates of the other events for the remainer of the same time step.

3.2 Modified KMC

We require a slight modification to include fixed-time death events. An additional check must be added after choosing the time step, to see which event will happen first: the next infection event or the next death event. If the death event will occur first, we discard the random time step and make the death event occur. This has a sound mathematical basis: the infection events are homogeneous Poisson processes, obeying $\mathrm{P}(t_{survive} > t_{infection}) = exp(-\lambda t)$, and are therefore memory-less [14].

Starting at time t_0, we have N possible events each with individual reaction rate λ_e, and the next death event will occur at t_{death}. Our modified KMC method is:

1. Calculate the cumulative infection rate function, $R(i) = \sum_{e=1}^{i} \lambda_e$
2. Choose a random number u in the range [0,1]. The next time of an infection is $t_{infection} = t_0 + ln(^1/_u)/R(N)$
3. If $t_{infection} > t_{death}$, then the death event occurs: set t_{death} as the new time; kill the node; recalculate the infection rates λ_e; and return to Step 1
4. Otherwise, choose a number v in the range [0,R(N)]. The event E that occurs is the one with $R(E-1) \leq v < R(E)$. Set $t_{infection}$ as the new time; infect the node; recalculate the infection rates λ_e; and return to Step 1

3.3 Improvements

The new method has given rise to a dramatic speed increase over the previous code: whereas the previous code could perform around 100 realisations per second [15], our code now performs at around 1000 realisations per second.

3.3.1 The std::map Container

The toy model used arrays and linear-search methods to store, access and edit the list of possible infection events. We now use the std::map class in C++ stdlib, which performs the same add/find/remove processes in much faster log(N) time (see e.g. [16]).

3.3.2 Retaining Cumulative Infection Rate

In our implementation, we now retain the total cumulative infection rate R(N) (see Section 3.2). Whenever any node's infection rate changes, we add or subtract from the retained cumulative rate. Step 1 in our modified KMC method is then irrelevant, and Step 2 can be performed instantly. There is some cause for concern over the finite precision of floating-point values [17], which occasionally introduces a small error. These errors are compounded when retaining R(N), since each addition/subtraction to R(N) introduces an extra small error. We performed a test on the accuracy of retaining R(N) by recalculating the cumulative infection rate R(N) at each KMC-step, and comparing it to the retained value. For a large world of size 500x500, the discrepancy was less than 10^{-14} which, compared to the standard infection rates of $\lambda \sim 0.5s^{-1}$, should be negligible. The only minor issue was when R(N) should be exactly zero (no possible events). We had to include a check at the beginning of the KMC step to account for this.

3.3.3 Entirely New Features

Our implementation includes some new features, many of which are crucial to the data that was gathered. We added Finite Rewiring Capability, allowing us to specify upper- and lower- bounds on the allowed radii of rewiring. We developed a Heuristic Function (see 4.1.1) that allows accurate and automatic estimation of the scale parameters. Video methods create visualisations of the infection's spread for debugging.

4 Methodology and Initial Tests

In this section, we give details of how data was gathered in order to determine the effect of network rewiring on the critical transmission rate α_c. We also performed some initial tests, primarily to check whether our new code generated the same data as before, but also to determine which data would be most interesting to gather.

4.1 The Critical Transmission Rate

The turnover from non-invasive to invasive infection occurs at the critical transmission rate α_c, such that infections with $\alpha > \alpha_c$ are invasive, and infections with $\alpha < \alpha_c$ are non-invasive. In particular, we are interested in $\alpha_c(\phi)$, the critical transmission rate as a function of the rewiring probability. This

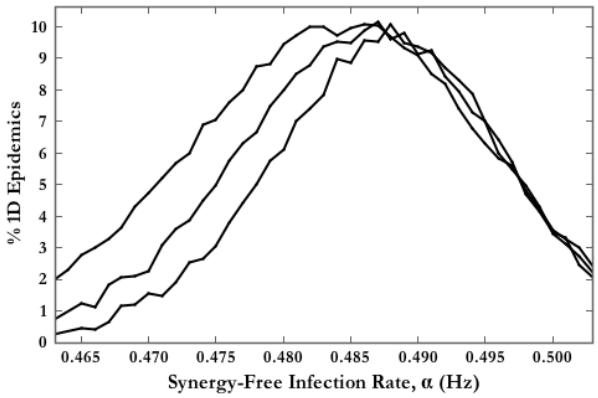

FIGURE 3: Finite Size Effects, showing the measured values of $N_1(\alpha)$ for Networks of size 91, 101, and 131

we approximate by determining α_c for several distinct values of ϕ. We use two independent processes to determine α_c for a single value of ϕ.

In the first method, we measure the Effective Mass of the infection as a function of the synergy-free infection rate α. As α is increased above the critical transmission rate, α_c, the Effective mass increases sharply and then shows a closely-linear fit [12]. In the second method, we perform a large number of realisations and measure the average fraction of 1-dimensional epidemics as a function of α, written as $N_1(\alpha)$. By finding $N_1(\alpha)$ for networks of different sizes L, we can perform finite size scaling to collapse the curves for different network sizes onto a single master curve. The scaling collapse gives us an estimate of α_c.

4.1.1 Finite Size Scaling

Networks of different sizes are expected ([6] Supplementary Notes) to generate slightly differing data sets $N_1(\alpha)$, because of finite size effects (see Figure 3). Data sets $N_1(\alpha)$ for different world sizes L should all collapse onto a single master curve when scaled according to

$$\alpha' = (\alpha - \alpha_c)L^{1/\nu} \tag{2}$$

and

$$N_1' = N_1 L^{-\theta} \tag{3}$$

where ν has a fixed value of 4/3 for a square lattice. The collapse is poor near the data tails, so we restrict our scaling analysis to data that are above $^2/_3$ of the data maximum. The problem has now been reduced to finding the values of α_c and

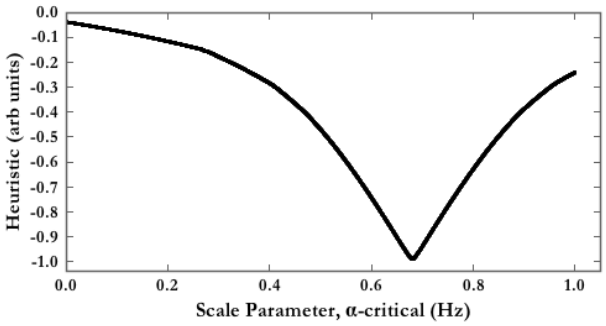

FIGURE 4: Heuristic Function against α_c – a clear minimum occurs at the theoretically best value of $ln(2) = 0.6931$

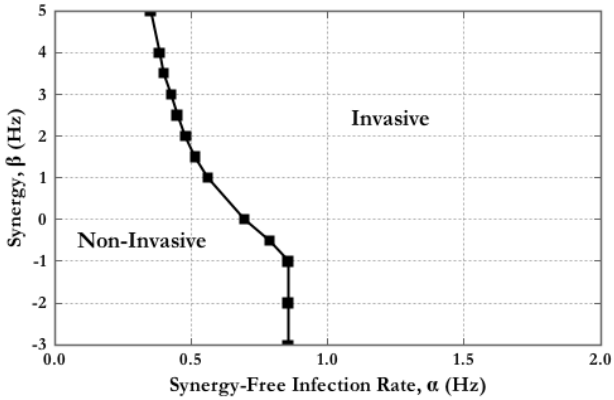

FIGURE 5: Phase Diagram, Synergy (β) against Critical transmission rate (α_c) for no network rewiring. Infections to the left of the line are non-invasive; infections to the right of the line are invasive.

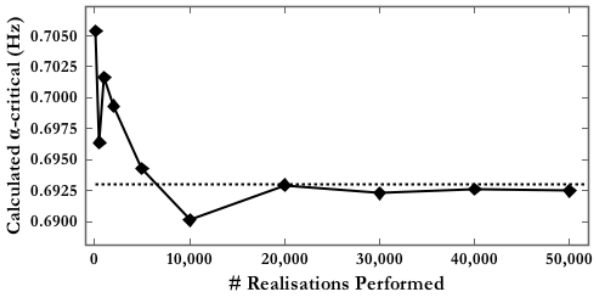

FIGURE 6: Estimated α_c against Number of Realisations. The dotted line shows the value of α_c from theory, $ln(2) = 0.6931$

θ that cause the best collapse. Although it is possible to find the best scale parameters by eye and using trial-and-error, it is much faster to quantify the collapse algorithmically and use standard minimisation methods to find the scale parameters that give the best collapse. We have developed a new Heuristic function that quantifies the goodness-of-collapse. The Heuristic function is calculated by scaling $N_1(\alpha)$ for all network sizes L, and then determining the overlap in areas between all pairs of sets. Figure 4 shows an example Heuristic function plotted against α_c. There is a clear minimum at the theoretically expected location.

4.2 Phase Diagram: α_c against β

Figure 5 show the critical transmission rate α_c for several β values with no rewiring. These were found using the 1d epidemics process, for five worlds of sizes near 111x111. These data gave a quick measure of whether the data being generated are correct. This diagram is identical to that found in the literature [6, 7].

4.3 Data Gathering

Each realisation is performed by rewiring the network using the rewiring probability ϕ, and then infecting the central node. Time then progresses using the KMC method above. Data for $N_1(\alpha)$ were gathered by first performing around 500 realisations over a sparse spread of α values, usually from $\alpha = 0.3$ to 0.7 taking step sizes of around 0.05. These data were used to determine the rough location and width of the curve. The range of α was then decreased so that we only included data points above $^2/_3$ of the peak height, to ensure the validity of Finite Size Scaling analysis (see Section 4.1.1) and to reduce any errors associated with including the data tails. The step size was also decreased until there were around 50-100 data points across the α range. Figure 6 shows how the number of realisations affects the accuracy of our α_c estimate for typical $N_1(\alpha)$ data. From this we estimate that 20,000 realisations is sufficient to give an accurate estimate of α_c, although 50,000 gives a safter estimate. Data for Effective Mass were gathered in a similar way, taking the range of α as the linear region with masses from 5 to 50.

5 Results

The data in this section were first derived as graphs of $\alpha_c(\phi)$ under various rewiring regimes. Figure 7 shows one such plot. For each value of the synergy β, the critical transmission rate α_c either increases or decreases with ϕ. By fitting a linear gradient to

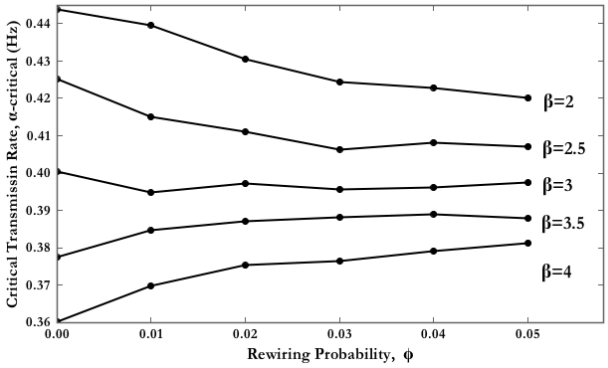

FIGURE 7: α_c vs ϕ for a few values of β under infinite rewiring regime. For each line, we measure the change in α_c over the range of ϕ, as a measure of the extent and direction in which α_c changes. The effective gradients are shown in Figure 8

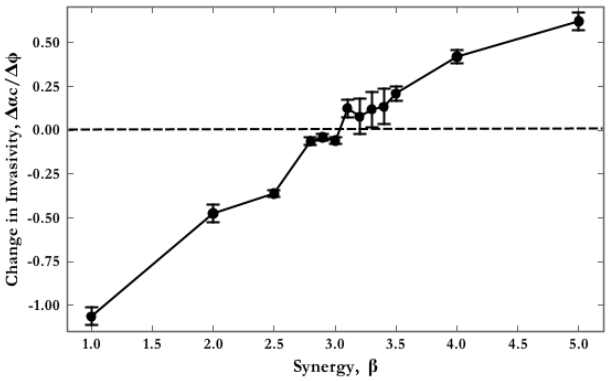

FIGURE 8: Effective-gradient $\Delta\alpha_c/\Delta\phi$ against β under infinite rewiring regime. The critical synergy value is at $\beta_c = (3.0 \pm 0.1)s^{-1}$. Error bars are calculated from the highest and lowest lines of best fit to the curves.

each line, we derived the value of $\Delta\alpha_c/\Delta\phi$, which we call the effective-gradient. We then plot these effective-gradients against the synergy β to demonstrate the direction and extent to which α_c changes for each value of β. Interpretations of the data are given afterwards in Section 6.

5.1 Infinite Rewiring

Figure 7 shows the effect of infinite network rewiring on α_c for several synergy values β. For low values of β, the critical transmission rate α_c decreases with rewiring probability ϕ. For high values of β, α_c increases with ϕ. Note that there are no error bars on this plot, since we only use it as a qualitative measure of the direction in which α_c changes over ϕ. Figure 8 shows the effective-gradients of the lines in Figure 7, calculated as the difference in the value of α_c divided by the change in ϕ over that range. The turn-over from decreasing- to increasing-α_c occurs at a critical value of $\beta_c = (3.0 \pm 0.1)s^{-1}$.

5.2 Finite Rewiring

Figure 9 shows the effect of finite network rewiring on the critical transmission rate. The effective-gradients $\Delta\alpha_c/\Delta\phi$ are plotted against β for two rewiring regimes: in the first, rewiring is restricted to between 5 and 10 lattice spacings; in the second, the limits are between 10 and 15 lattice spacings. We observe the same effect as was seen for infinite rewiring, namely that there is a critical value of synergy, β_c, at which the effective-gradient of $\alpha_c(\phi)$ changes from negative to positive. recall that a positive effective-gradient means that the critical transmission rate increases with the extent of rewiring. For finite rewiring between 5 and 10 lattice spacings, we observed $\beta_c = (2.0 \pm 0.1)s^{-1}$. For finite rewiring between 10 and 15 lattice spacings, we observed $\beta_c = (2.5 \pm 0.1)s^{-1}$.

5.3 Infinite Rewiring, without bond destruction

Figure 10 shows $\alpha_c(\phi)$ for a large synergy of $\beta = 10$. Under the normal infinite rewiring regime, the α_c increases with ϕ as before. However, when rewiring is performed by only adding bonds (and not removing any – see Section 2.1.2), the effect is removed. An interpretation of why this is the case is given in the next section.

6 Discussion

We have observed that infections exhibiting large positive synergy benefit from rewiring. Our interpretation of this feature relies on the two opposing effects that rewiring has on a network: the benefit, and the cost, of following a shortcut to a new region of the network. We shall also compare the "stability" of regions within the network: the stability of a region is the extent to which the infection finds it easier to spread there.

6.1 Rewiring and Stability

First, consider the obvious benefit gained from following shortcuts. Shortcuts allow an infection to

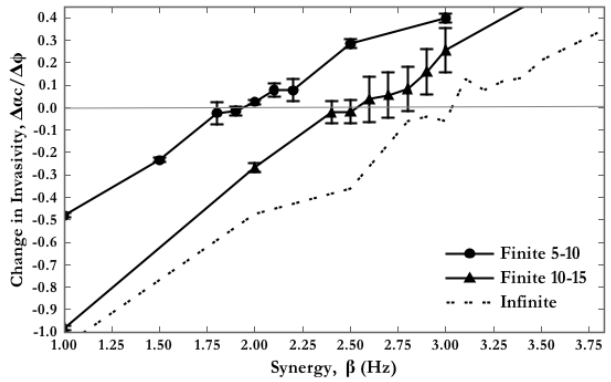

FIGURE 9: Effective-gradients $\Delta\alpha_c/\Delta\phi$ against β for two rewiring regimes: 5-10 lattice spacings (circles) and 10-15 lattice spacings (triangles). The critical synergy values are $\beta_c = (2.0 \pm 0.1)s^{-1}$ and $\beta_c = (2.5 \pm 0.1)s^{-1}$, respectively. The dotted line shows the data from Figure 8 for infinite rewiring. Note the larger error bars for the 10-15 regime, since these values of beta were run only up to 10,000 realisations owing to time constraints.

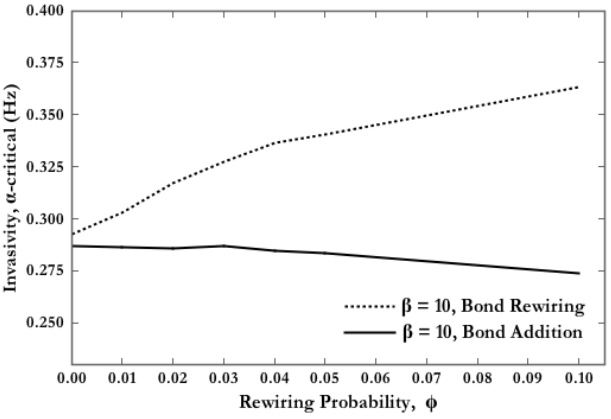

FIGURE 10: α_c vs ϕ for $\beta = 10.0$ using infinite-length shortcuts. The dotted line shows the effect of network rewiring (adding and removing one bond per rewiring event); the solid line shows the effect of only adding bonds. The effects are clearly very different.

jump into a new region, one which is not directly adjacent to the central cluster. By jumping into a fresh and untouched region of the network, the infection has a larger number of susceptible hosts and a larger susceptible region into which it may grow. Overall, this effect causes the infection spread more easily across the whole network. We shall refer to this effect as the Benefit Effect of shortcuts.

Secondly, consider the possible cost of taking a shortcut. When an infection follows a shortcut, it does so instead of infecting one of its adjacent neighbours. Figure 1 shows this more clearly: whenever a shortcut bond is created, a local bond is destroyed. The shortcut literally replaces the bond to the adjacent node, so that the distant node is infected instead of the adjacent node. This only affects the spread of the infection if the local region is more stable (recall the use of "stability" above) than the region into which the shortcut leads. In other words, this effect only exists if the infection rate is affected by the environment into which it the infection is transmitted – this is exactly the definition of synergy. For positive synergy, the local region (near the base of the shortcut) is more stable than the distant region (at the end of the shortcut), since the local region is likely to have many more nearby infected hosts. We shall refer to this effect as the Cost Effect of shortcuts.

6.2 Infinite Rewiring

For infinite rewiring, it is most likely that shortcuts will lead to very distant regions from the central cluster, because most of the area of a circle lies at its periphery. The Benefit Effect is strong for infinite rewiring. but what about the Cost Effect? Consider separately the cases and no synergy, and positive synergy.

For an infection exhibiting no synergy, the stability of the local region is exactly the same as the stability of the distant region. Any individual infected host is unaffected by the presence (or absence) of other nearby infected hosts. Thus, following a shortcut bond is effectively the same as following an adjacent bond. The Benefit Effect dominates over the non-existent Cost Effect, and the infection finds it easier to spread when there is more rewiring. This is as observed: the critical transmission rate α_c decreases with larger rewiring probability ϕ. Equivalently, the effective-gradient $\Delta\alpha_c/\Delta\phi$ is negative for $\beta = 0$.

For an infection exhibiting positive synergy, an infected host benefits strongly from the presence

of other nearby infected hosts. The transmission rate with which it infects its susceptible neighbours (Equation 1, $\lambda = \alpha + \beta(n_{defender} - 1)$) is greatly enhanced if there are other nearby infected hosts. Thus, following a shortcut bond is significantly worse than following a bond to an adjacent node. For low synergy, the Benefit Effect still dominates and the effective-gradient $\Delta\alpha_c/\Delta\phi$ remains negative. As the synergy is increased, the Cost Effect grows in strength. At a critical value of synergy, the Benefit and Cost Effects are balanced and the infection is unaffected by the extent of rewiring. Above the critical value, the Cost Effect is stronger and the infection spread is hindered by the increased rewiring.

6.3 No Bond Destruction

Further justification for our interpretation of stability comes from Figure 10. This figure shows what happens for large synergy when no bonds are destroyed during the rewiring process. That is, instead of rewiring the bonds we simply add new bonds to the network. The Cost Effect is greatly reduced and we even observe the Benefit effect slightly dominating: the additional shortcuts only increase the number of possible infection events. The infection appears to remain at a fairly constant value of $\beta = (0.28 \pm\ 0.05)s^{-1}$.

6.4 Finite Rewiring

Before this study, it was unclear whether the same effect would be seen in radius-limited rewiring. Both the Benefit and the Cost Effects are dependent on the range of rewiring radii.

The Benefit Effect is more pronounced the further away the infection can travel. This can be seen by observing what happens at low synergy ($\beta \approx 1$) on Figure 9. The Benefit Effect is much more pronounced for rewiring in the range 10-15 than it is for rewiring between 5-10, as can be seen by the magnitude of $\Delta\alpha_c/\Delta\phi$. Likewise, $\Delta\alpha_c/\Delta\phi$ is slightly larger in magnitude for Infinite rewiring than it is for rewiring in the range 10-15.

The Cost Effect is also affected by the rewiring radii, as can be seen by the fact that the two curves for 5-10 and 10-15 approach one another at larger synergy. When the infection can only jump short distances, we might expect the "distant" region to be of similar stability to the local region. Thus the Cost Effect is thus stronger for larger rewiring radii, as observed.

We would expect both patterns to continue as the radii of the regions are increased further.

7 Conclusions

The results of this paper show that the spread of a cooperative infection can be obstructed by using network rewiring. This result can be understood in the context of rumours in social groups. If there is strong cooperation between nearby members of the group, it would be sensible to force the group to spread out in the world or, equivalently, somehow prevent nearby members from discussing the rumour (i.e. bond destruction).

The critical value at which this effect is observed depends on the radius of rewiring shortcuts. For infinite rewiring, the critical synergy occurs at $\beta_c = (3.0 \pm\ 0.1)s^{-1}$. For finite rewiring between 10 and 15 lattice spacings, the critical synergy occurs at $\beta_c = (2.5 \pm\ 0.1)s^{-1}$. For finite rewiring between 5 and 10 lattice spacings, the critical value occurs at $\beta_c = (2.0 \pm\ 0.1)s^{-1}$. These values can also best be understood in the context of rumours. The further apart we separate the members of the group (i.e. longer shortcuts), the less support they have from their cooperative neighbours, and the less easy they will find it to continue spreading the rumour.

7.1 Further Work

Several features of our data would be interesting to investigate further. First, it would clearly be interesting investigate larger rewiring radii limits, and see the point at which the small-world network assumption breaks down. We would expect the trend of increasing β_c to continue for larger rewiring radii.

Secondly, it would be interesting to quantify the stability of various regions. One method of this might be to determine the average length of bonds between neighbours under the various rewiring regimes. The longer the average bond, the further afield the shortcuts take the infection, and the less likely it is that the distant region is supported by the main cluster's infected hosts.

Thirdly, we have concentrated on the synergy region near β_c, where the behaviour of the critical transmission rate α_c changes. It might be interesting to investigate what happens at higher and lower synergy values, and at much higher rewiring probabilities. At much higher rewiring probability, we would predict that Finite size effects would be much more pronounced.

Finally, we have ignored any analysis of the θ scale parameter. This parameter quantifies the extent to which larger worlds give rise to a smaller peak in the value of N_1, and we would expect it to show some relationship with rewiring probability. Unfortunately, the quantity of data needed to give an accurate value of θ was unfeasibly high, and beyond the scope of this study.

References

[1] DIETER SCHENZLE. An age-structured model of pre- and post-vaccination measles transmission. *IMA Journal of Mathematics Applied in Medicine Biology*, 1:169–191, 1984.

[2] WAYNE P. LONDON and JAMES A. YORKE. Recurrent outbreaks of measles, chickenpox and mumps. *AMERICAN JOURNAL of EPIDEMIOLOGY*, 98:453–468, 1978.

[3] Bryan T. Grenfell Matt J. Keeling, Pejman Rohani. Seasonally forced disease dynamics explored as switching between attractors. *Physica D: Nonlinear Phenomena*, 148: 317–335, 2001.

[4] Maziar Nekoveeb Valerie Ishama, Simon Hardena. Stochastic epidemics and rumours on finite random networks. *Physica A: Statistical Mechanics and its Applications*, 389, 2010.

[5] DEPARTMENT OF AGRICULTURE, RURAL DEVELOPMENT, AGRI-FOOD, and BIOSCIENCES INSTITUTE. Contingency plan for exotic pests and diseases of honey bees for northern ireland, 2013.

[6] Sergei N. Taraskin and Francisco J. Perez-Reche. Effects of variable-state neighborhoods for spreading synergystic processes on lattices. *Phys. Rev. E*, 88:062815, Dec 2013. doi: 10.1103/PhysRevE.88.062815. URL `http://link.aps.org/doi/10.1103/PhysRevE.88.062815`.

[7] Francisco J. Pérez-Reche, Jonathan J. Ludlam, Sergei N. Taraskin, and Christopher A. Gilligan. Synergy in spreading processes: From exploitative to explorative foraging strategies. *Phys. Rev. Lett.*, 106:218701, May 2011. doi: 10.1103/PhysRevLett.106.218701. URL `http://link.aps.org/doi/10.1103/PhysRevLett.106.218701`.

[8] Steven H. Strogatz Duncan J. Watts. Collective dynamics of small-world networks. *Nature*, 393:440–442, 1998.

[9] W. OTTEN D. J. BAILEY and C. A. GILLIGAN. Saprotrophic invasion by the soil-borne fungal plant pathogen rhizoctonia solani and percolation thresholds. *New Phytologist*, 146: 535–544, 2000.

[10] Samuel R. Friedman, Benny J. Kottiri, Alan Neaigus, Richard Curtis, Sten H. Vermund, and Don C. Des Jarlais. Network-related mechanisms may help explain long-term hiv-1 seroprevalence levels that remain high but do not approach population-group saturation. *American Journal of Epidemiology*, 152(10): 913–922, 2000. doi: 10.1093/aje/152.10.913.

[11] M. E. J. Newman and D. J. Watts. Scaling and percolation in the small-world network model. *Physics Review*, 60:7332–7342, 1999.

[12] I.M. Sokolov C.Simon J.Koopman L. M. Sander, C.P. Warren. Percolation on heterogeneous networks as a model for epidemics. *Mathematical Biosciences*, 180: 293–305.

[13] R. Peierls. Statistical error in counting experiments. *Series A, Mathematical and Physical Sciences*, 149-868:467–486, 1935.

[14] Francisco J. Perez-Reche. Private correspondence.

[15] Dr S. N. Taraskin. Private correspondence.

[16] http://www.cplusplus.com/reference/map/map/find/.

[17] Eric Goubault and Sylvie Putot. Static analysis of finite precision computations.